

Stylized Aesthetic QR Code

Mingliang Xu , Hao Su , Yafei Li , Xi Li , Jing Liao, Jianwei Niu , Pei Lv , and Bing Zhou

Abstract—With the continued proliferation of smart mobile devices, the *Quick Response (QR)* code has become one of the most-used types of two-dimensional code in the world. Aiming at beautifying the visual-unpleasant appearance of QR codes, existing works have developed a series of techniques. However, these works still leave much to be desired, such as personalization, artistry, and robustness. To address these issues, in this paper, we propose a novel type of aesthetic QR codes, *Stylized aEsthetic (SEE) QR code*, and a three-stage approach to automatically produce such robust style-oriented codes. Specifically, in the first stage, we propose a method to generate an optimized baseline aesthetic QR code, which reduces the visual contrast between the noise-like black/white modules and the blended image. In the second stage, to obtain an art style QR code, we tailor an appropriate neural style transformation network to endow the baseline aesthetic QR code with artistic elements. In the third stage, we design a module-based robustness-optimization mechanism to ensure the performance robust by balancing two competing terms: visual quality and readability. Extensive experiments demonstrate that the *SEE QR code* has high quality in terms of both visual appearance and robustness and also offers a greater variety of personalized choices to users.

Index Terms—QR code, style-oriented, visual aesthetics, robust.

I. INTRODUCTION

WITH the continued proliferation of the internet and smart mobile devices, the *Quick Response (QR)* code has become one of the most widely used information carriers in the world. However, the ordinary QR codes have visual-unpleasant appearances and consist of monotonic black/white square

Manuscript received April 22, 2018; revised November 26, 2018; accepted December 19, 2018. Date of publication January 7, 2019; date of current version July 19, 2019. This work was supported in part by the National Natural Science Foundation of China under Projects 61822701, 61602420, 61672469, 61472370, 61772474, and 61872324, in part by the National Key R&D Program of China under Project 2017YFC0804401, in part by the China Postdoctoral Science Foundation through Project 2018M630836, in part by the Supporting Plan for Scientific and Technological Innovative Talents in Universities of Henan Province under Project 18HASTIT020, and in part by the Training Plan of Young Key Teachers in Colleges and Universities of Henan Province under Project 2016GGJS-001. The associate editor coordinating the review of this manuscript and approving it for publication was Dr. Marco Bertini. (*Corresponding author: Yafei Li*)

M. Xu, H. Su, Y. Li, P. Lv, and B. Zhou are with Zhengzhou University, Zhengzhou 450066, China (e-mail: iexumingliang@zzu.edu.cn; suhao@gz.zzu.edu.cn; ieyfli@zzu.edu.cn; ielvpei@zzu.edu.cn; iebzhou@zzu.edu.cn).

L. Xi is with Zhejiang University, Hangzhou 310027, China (e-mail: xilizju@zju.edu.cn).

J. Liao is with Microsoft Research Lab—Asia, Beijing 100080, China (e-mail: jliao@microsoft.com).

J. Niu is with Beihang University, Beijing 100083, China (e-mail: niujianwei@buaa.edu.cn).

This paper has supplementary downloadable material available at <http://ieeexplore.ieee.org/>, provided by the authors. The material includes Appendices A, B, and C. This material is 3 MB in size.

Color versions of one or more of the figures in this paper are available online at <http://ieeexplore.ieee.org>.

Digital Object Identifier 10.1109/TMM.2019.2891420



Fig. 1. Four types of existing approaches to beautify the QR codes.

modules which are meaningless to human vision. Hence, the visual optimization of QR code has attracted extensive attentions from academia and industry.

As shown in Fig. 1, existing works can be categorized into four types: i) *embedded-type* [1]–[5] which embeds small icons utilizing the error-correction capability of QR codes; ii) *deformation-type* [5] that changes the shape and color of the modules in QR codes, e.g. turning the square modules into round, triangle, star; iii) *manual type* [5] which is produced by manual design and rendering; iv) *blended-type* [6]–[13] which blends a large image into QR code. Among these, the *blended-type* is considered as the most promising technique for generating QR codes with the highest visual quality.

Although existing works have improved the visual quality of QR code to some extent, they still leave much to be desired in terms of the following three aspects: i) **Personalization**, mainstream works generate aesthetic QR codes with different appearances via changing the blended images. In fact, users always expect to produce personalized aesthetic QR codes in different styles by a unique blended image (e.g. logo, personal photo or trademark). ii) **Artistry**, most existing works define “beauty” is “more similar to the blended image”, they produce QR codes by combining an image with black/white modules directly, which lacks additional aesthetic refinement. Moreover, their resultant modules are always invariable and mechanical even blended with beautified images [cf. Fig. 4(a)–(d)]. iii) **Robustness**, some current works lack a method to check whether there exist error modules in outputs, and some other works even covering QR codes’ parity bits with an image. Therefore, in complex real scenarios, smearing few modules may exceed the QR codes’ error-correction capability, which results in unreadable.

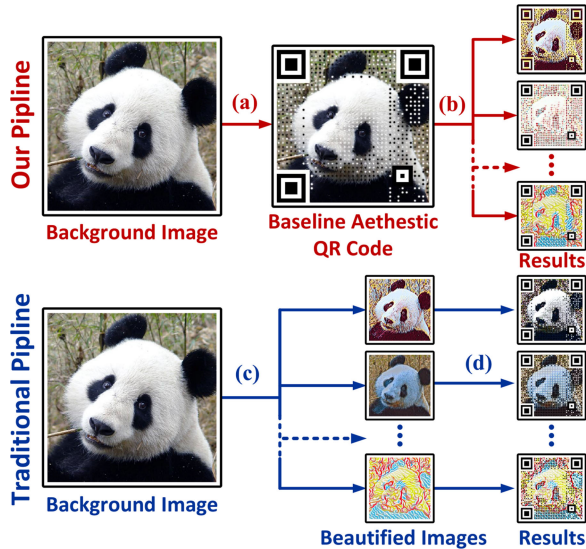


Fig. 2. Two pipelines to produce art style aesthetic QR codes. (a) and (b) Our approach stylizes the baseline aesthetic QR code to generate art style results. (c) and (d) Traditional blended-type methods need first stylize the blended images and then add black/white encoding modules. In fact, traditional results are still baseline aesthetic QR codes that only blend with artistic images [cf. Fig. 4(a)–(d)]. Compared with the traditional pipeline, our approach has two merits: i) we further beautify encoding modules’ appearances [cf. Fig. 4(e)–(l)]. ii) The image and modules are deeper blended into a unified style while enhancing the visual appeal.

Solving any of these issues without compromising other properties is a big challenge. In this paper, we propose an effective approach to automatically produce robust art style QR code, called *SEE (Stylized aEsthetic) QR code*, by leveraging the CNN-based style transformation network. As shown in Fig. 3, SEE QR codes are style-oriented aesthetic codes that can be produced with various personalized styles by blending a single image. Moreover, our approach directly stylizeds the baseline aesthetic QR code [cf. Fig. 2(a) and (b)], which endows the encoding modules and blended image with unified artistic elements and enhances their visual appeal [cf. Fig. 4(e)–(l)]. Finally, we design a module based robustness-optimization mechanism to ensure each module’s robustness, by balancing two competing items, visual quality, and readability.

To summarize, our main contribution in this paper is fourfold:

- We propose a new type of aesthetic QR codes, SEE QR code, which is personalized, artistical, and robust.
- We design an efficient algorithm for scheduling changeable modules in baseline aesthetic QR codes, which minimizes the visual contrast between black/white encoding modules and the blended image.
- We adapt a style transfer network for stylizing the baseline aesthetic QR codes, which effectively avoids the visual affecting of noise-like modules while reduces the encoding message loss during the transformation.
- We present a module based robustness-optimization mechanism that can independently check and repair each module’s robustness by balancing two competing items, visual quality, and readability.

II. RELATED WORK

In this section, we review techniques related to our work which mainly refer to two topics, aesthetic QR code and style transfer.

A. Aesthetic QR Code

As elaborated in Section I, up to now, the manual-type techniques are high-cost and non-automatic, the embedded-type techniques and deformation-type techniques have unideal visual effect. In contrast, the blended-type techniques with good visual quality are the most promising approach that deserves further study. The details about representative existing blended-type works are as follows.

Peled *et al.* [6] developed a visual QR code generator called *Visualead* [cf. Fig. 5(a)] which retains the original contrast between the encoding modules and the blended image to synthesize the aesthetic QR codes. However, the QR codes generated by the *Visualead* have serious artifacts that notably reduce the visual content of the blended image.

Inspired by the technique of halftone, Chu *et al.* [7] presented a novel style aesthetic QR code called halftone QR codes [cf. Fig. 5(b)]. The idea of generating halftone QR codes is that they subdivide each module of the standard QR code into 3×3 submodules and bind the module’s color to the center submodule while the remaining 8 submodules are modified to balance the reliability and regularization.

Aiming at blending image to a full-size area of the QR code, Lin *et al.* [8] synthesize aesthetic QR code based on the Gauss-Jordan elimination used in the QArt method [14] and improve the visual quality by a rendering mechanism, which is combined by the techniques of embedded-type and blended-type. Such QR code is suitable for the blending image of which saliency content is in images’ center and not near the edges [cf. Fig. 5(c)].

Leveraging QArt method [14], Zhang *et al.* [10] relocated the modules of QR code that depend on the visual saliency and edge features extracted from blended image [cf. Fig. 5(d)]. This approach tends to distribute the black/white modules in the visual focus area, and output QR codes with visual-pleasant. However, this approach lacks an error correction mechanism to ensure the readability, and it is still improvable in the perspective of visual quality by adopting the image’s global feature.

B. Style Transfer

Recently, style transfer has become a hot research topic in AI field, which is very related to texture synthesis. It can be interpreted as migrate artistic style from a style target image and blended with semantic information of the content target image.

Early studies on style transfer can be divided into two primary types: one type is based on optimization [15], [16], it produces impressive stylized image but is too time consuming for iterative optimizing; the other type is based on feed-forward network [17], [18], feed-forward generator network is trained for each specific style target image, the original time-consuming



Fig. 3. Some examples of our SEE QR code, which are personalized, artwork-like, and machine-readable. Moreover, users can produce them in various visual-pleasant styles via a single blended image.

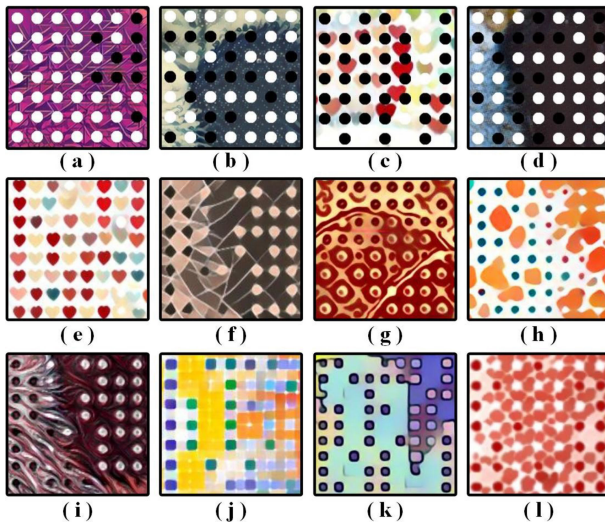


Fig. 4. (a)-(d) Encoding modules in the results of traditional pipeline (cf. Fig. 2), which have noise-like invariable appearances. (e)-(l) Encoding modules in our SEE QR code (cf. Fig. 2), where the blended images and modules are simultaneously endowed with attractive artistic elements in a unified style.

iterative optimization is replaced by a forward pass mechanism. Moreover, the learned style transfer feed-forward networks can output the results nearly real-time.

After that, Chen *et al.* [19] proposed an efficient method named StyleBank that allows a single network to simultane-

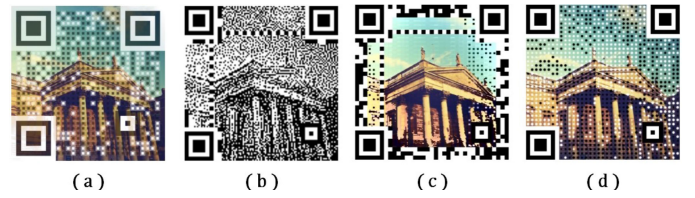


Fig. 5. Representative blended-type existing works on aesthetic QR codes. (a) Visualead QR code [6]. (b) Halftone QR code [7]. (c) Efficient QR Code [8]. (d) Two-Stage based QR code [10].

ously learn numerous styles. StyleBank is composed of multiple convolution filter banks, each filter bank explicitly represents one style for neural image style transfer. Based on this mechanism, style transfer can be realized through using StyleBank and auto-encoder.

Liao *et al.* [20] proposed a novel technique called deep image analogy for visual attribute transfer. They combine the techniques of image correspondence and neural style transfer, and achieves prominent visual effect through establishing a pixel-level correspondence between two images which have similar semantic structure and different appearances.

In this paper, we first combine the techniques of aesthetic QR code and style transfer to generate a novel type of art style QR codes which are personalized, diversified, artistic and machine-readable.

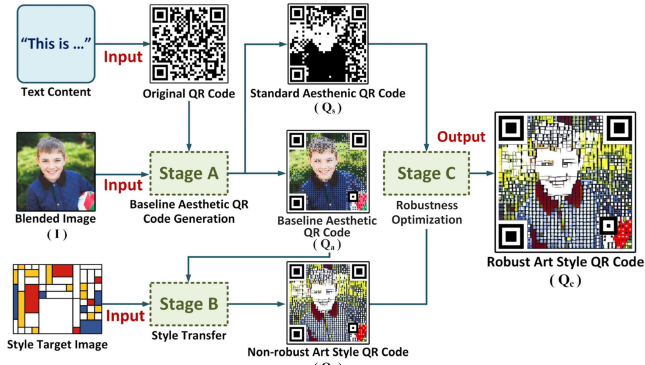


Fig. 6. Overview of our approach, which consists of three stages: Stage A: baseline aesthetic QR code generation, Stage B: style transfer, and Stage C: robustness optimization.

TABLE I
SUMMARY OF NOTATIONS

Name	Description
I	The input image used for blending.
Q_s	The standard QR code produced in Stage A.
Q_a	The baseline aesthetic QR code produced in Stage A.
Q_b	The non-robust art style QR code produced in Stage B.
Q_c	The robust art style QR code produced in Stage C, namely SEE QR code.
Q^g	The grayscale image of QR code Q .
Q^b	The binary image of QR code Q .
Q^c	The color image of QR code Q .
Q^t	The threshold of QR code Q .
Q_x	The x -th pixel of QR code Q .
M_k	The k -th encoding module of QR code.
$S_{(k,r)}$	The k -th circular encoding spot of radius r and concentric with M_k .

III. OVERVIEW OF OUR APPROACH

As shown in Fig. 6, our approach is consist of three stages denoted as Stage A, Stage B, and Stage C. Initially, depending on a novel strategy of scheduling changeable modules, we produce an optimized baseline aesthetic QR code Q_a , in Stage A. Then in Stage B, to endow Q_a with artistic elements while considering the particularity of QR codes, we adapt a neural style transfer network for stylizing Q_a and obtain an art style QR code Q_b . Finally, in Stage C, aiming at eradicating error modules in Q_b to ensure the readability, a module based robustness-optimization mechanism is presented to check and repair all error modules for outputting a robust art style result Q_c .

The details of Stage A, Stage B, and Stage C will be introduced in the following three Sections respectively. Table I summarizes the notations used throughout this paper.

IV. STAGE A: AESTHETIC QR CODE GENERATION

A. Basic of Stage A

QR code is based on the coding rules of Reed-Solomon (RS) code and expressed as square encoding modules. Cox [14]

proved that *Gauss-Jordan Elimination Procedure* (GJEP) can be employed to schedule changeable modules in a limited range without compromising the machine readability.¹

Mainstream works (e.g. [7]–[11]) always manipulate the GJEP to schedule the changeable modules by considering blended images' local visual features, such as saliency map, edge map, or ROI (region of interesting). Unlike them, in Stage A, we propose an effective strategy that depends on the global gray values of blended image I and produces a baseline aesthetic QR code Q_a , which minimizes the visual contrast between I and the noise-like black/white modules.

In the grayscale blended image I^g , the gray value of each pixel is in $[0, 255]$ while that of the black and white modules are constant 0 and 255 respectively. Accordingly, the visual contrast is minimized when the gray value of module is most approximate to that of the corresponding pixels in I^g . In other words, when the pixels in I with the darkest/lightest color are preferentially scheduled with black/white module, the visual performance of Q_a will be improved a lot.

B. Generating Process

In this paper, we utilize the QR code of version 5 and error correction level L as the default setting. We first generate a grayscale copy I^g of I , and divide I^g into $m \times m$ modules of size $a \times a$ pixels, which adheres to the ISO standard [21]. W_{M_k} denotes the normalized priority weight of scheduling module M_k , which is defined as

$$W_{M_k} = \frac{1}{W_m} \sum_{x \in M_k} W_x , \quad (1)$$

where x is a pixel of module M_k , W_x is the weight of x with a maximum value of W_m , for the convenience of calculation, here $W_m = 255$. We assign all pixels with different weights W_x and minimize the following energy function to automatically calculate the best W_x for each pixel

$$E = \sum_{x \in \{1, 2, \dots, (a \cdot m)^2\}} \left\{ \|(Q_s)_x^g - I_x^g\|^2 \times G_{M_k}(x) + \|W_m - [W_x + \|(Q_s)_x^g - I_x^g\|^2 \times G_{M_k}(x)]\|^2 \right\} , \quad (2)$$

where $(Q_s)_x^g$ is 0 or 255. The first term in the summation ensures that the gray value of each pixel in the resultant standard QR code Q_s should be similar to I^g . The second term in the summation ensures that pixels with smaller gray value differences are assigned higher weights. $G_{M_k}(x)$ denotes a *Gaussian weight function* we defined, due to the rule that the pixels closer to the center with higher probability to be sampled during scanning, $\sum_{x \in M_k} G_{M_k}(x) = 1$. Here,

$$G_{M_k}(x) = G_{M_k}(i, j) = \frac{1}{2\pi\sigma^2} e^{-\frac{i^2+j^2}{2\sigma^2}} , \quad (3)$$

where i, j respectively denote the horizontal-ordinate and vertical-ordinate of pixel x when setting up a coordinate system

¹The theorem of scheduling modules can be found in Appendix A.

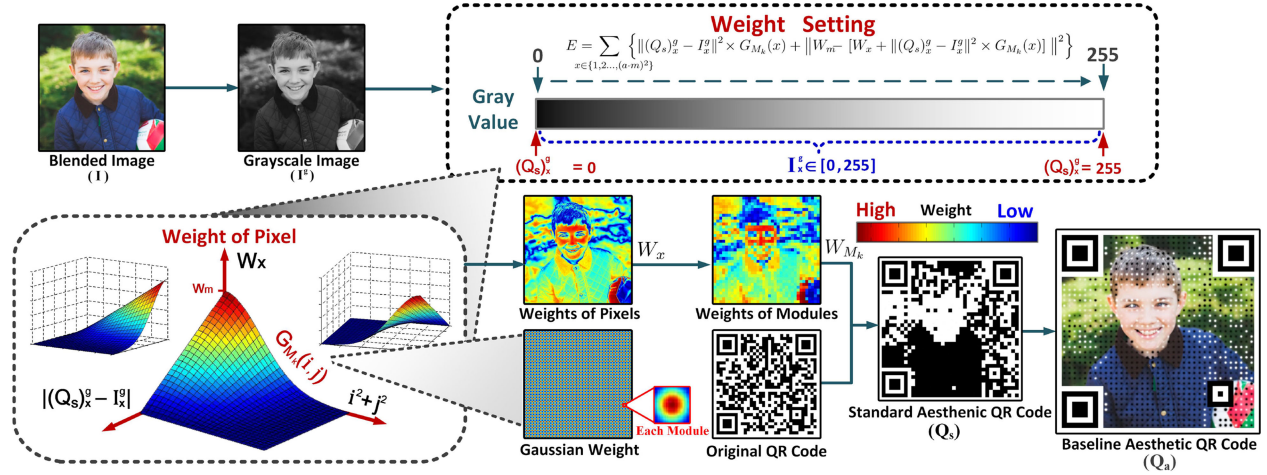


Fig. 7. Flowchart of Stage A. We calculate the priority weights of scheduling changeable modules depend on the gray value distribution of the blended image. This method can minimize the visual contrast between the blended image and noise-like black/white modules, which end up with a baseline aesthetic QR code Q_a .

with an origin at the center of M_k . In Gaussian weight function, pixels' weights are reduced to 0 when the distance between pixels and the center of Gauss template is greater than 3σ , and the Gauss template of size $(6\sigma + 1) \times (6\sigma + 1)$ can effectively reflect the relationship between the surroundings and the center pixels. Here, the Gauss template is the module M_k whose side length is a , thus we set $\sigma = \frac{a-1}{6}$ for easy calculation.

According to Eq. (1) and Eq. (2), the weight of each module in I^g is calculated to obtain an $m \times m$ weight matrix W . For the k -th module with a bigger weight, we give higher priority to it for being scheduled a module which has the same binary result as the k -th module of I^g , that is,

$$(Q_s)_{M_k}^b = \text{Round} \left\{ \left[\sum_{x \in M_k} I_x^g \cdot G_{M_k}(x) \right] \times \frac{1}{255} \right\}, \quad (4)$$

where $(Q_s)_{M_k}^b$ is 0 or 1, the function $\text{Round}\{\}$ indicates that rounding parameters inside braces to the nearest integer. Afterward, according to W , we manipulate *Gauss-Jordan elimination procedure* mentioned in [14] to schedule changeable modules in original QR code and produce the standard aesthetic QR code Q_s .

Finally, we replace the black/white square modules M_k of Q_s with circular spots $S_{(k,r)}$ of radius $\frac{1}{4}a$ (the setting of $S_{(k,r)}$ will be detailed in subsection B, Section VI) and fill the rest area with the corresponding pixels of I , thus the baseline aesthetic QR code Q_a is produced.

V. STAGE B: STYLE TRANSFER

A. Framework of Style Transfer System

Fig. 8 shows our system framework of the style transfer that roughly follows the architecture proposed in [17]. It is composed of two primary parts: a pretrained loss network ϕ and a deep residual convolutional neural network f_W .

In this system, ϕ is the 16-layer VGG network [22] pretrained on ImageNet [23]. f_W is used for transforming image x into image $\hat{a} = f_W(x)$, which is trained by

stochastic gradient descent to minimize a weighted combination of loss functions

$$W^* = \arg \min_W E_{x, \{a_i\}} \left[\sum_{i=1} \lambda_i l_i(f_W(x), a_i) \right], \quad (5)$$

where λ_i is a scalar, and each loss function $l_i(\hat{a}, a)$ is defined by ϕ to measure the difference between the output image \hat{a} and a target image a_i . $l_i(\hat{a}, a)$ specifically contains a feature reconstruction loss l_{feat}^ϕ and a style reconstruction loss l_{style}^ϕ , defined as

$$\begin{aligned} l_{feat}^{\phi,j}(\hat{a}, a) &= \frac{1}{C_j H_j W_j} \|\phi_j(\hat{a}) - \phi_j(a)\|_2^2, \\ l_{style}^{\phi,j}(\hat{a}, a) &= \|G_j^\phi(\hat{a}) - G_j^\phi(a)\|_F^2 \end{aligned} \quad (6)$$

where $\phi_j(x)$ is a feature map extracted from the j -th convolutional layer of network ϕ when x as the input, C_j , H_j , and W_j express the channel number, the height, and the width of $\phi_j(x)$ respectively. $G_j^\phi(x)$ is a defined *Gram matrix* of size $C_j \times C_j$ whose elements are given by

$$G_j^\phi(x)_{c,c'} = \frac{1}{C_j H_j W_j} \sum_{h=1}^{H_j} \sum_{w=1}^{W_j} \phi_j(x)_{h,w,c} \cdot \phi_j(x)_{h,w,c'}. \quad (7)$$

Once the training process of f_W is finished, we can use f_W to transform the input images Q_a into stylized results Q_b in real-time.

B. Adaptability Adjustment of Network

In Stage B, when the baseline aesthetic QR code Q_a with dense black/white encoding modules are treated as the content target of the style transfer, two key issues for consideration: i) For the robustness, the loss of encoding messages incurred by style transformation should be minimized; ii) For the visual quality, avoiding the visual damage caused by the noise-like modules is necessary. Aiming at these goals, we carry out the following tasks.

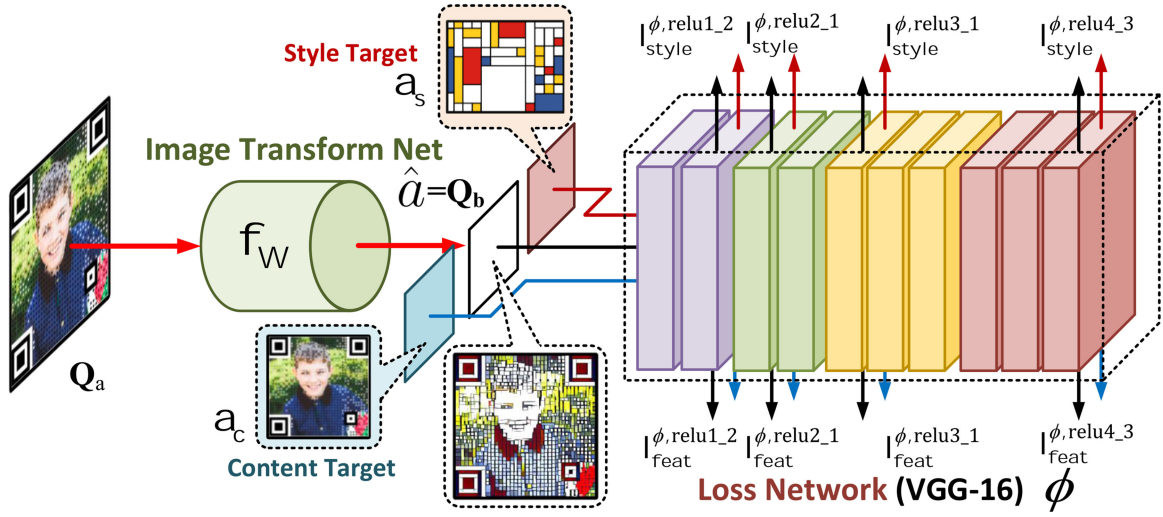


Fig. 8. Flowchart of Stage B. We roughly follow the style transfer system proposed by [17]. Aiming at enhancing the adaptability for stylizing baseline aesthetic QR codes which have dense black/white modules, we further adapt the layers of reconstructing style/content features loss in the loss network ϕ , and finally produce non-robust art style QR code Q_b .

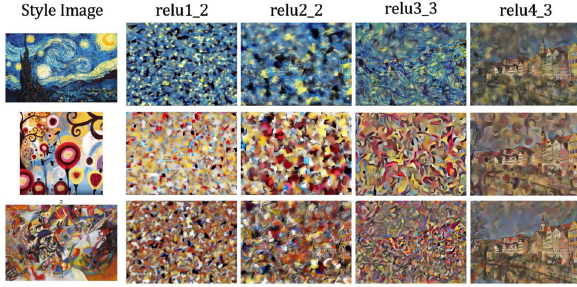


Fig. 9. We evaluate the style features reconstructed from the pretrained VGG-16 loss network in layers relu1_2 , relu2_2 , relu3_3 and relu4_3 . We find that the features reconstructed from low-level layers extremely similar to the dense encoding modules of aesthetic QR codes, which inspired us.

Initially, as illustrated in Fig. 9, we evaluate the style features reconstructed from layers relu1_2 , relu2_1 , relu2_2 , relu3_1 , relu3_2 , relu3_3 , relu4_1 , relu4_2 , relu4_3 of the pre-trained VGG-16 loss network ϕ . Afterward, we find that in lower layers (e.g., relu1_2 and relu2_2), the reconstructed style features put more emphasis on localization that presents as discrete textures and dense fragments, which is extremely similar to the encoding modules of Q_a . Correspondingly, with the increasing of the layers in VGG-16, the reconstructed features are gradually changed from localization to globalization. These phenomena inspired us.

Consider the special characteristics of Q_a (i.e., Q_a has discrete, fragmented, and dense encoding modules), as shown in Table II, we pertinently adapt the loss reconstruction layers of the style/content features. As expected, after the modification, we obtain desired results² on both visualization and robustness.

VI. STAGE C: ROBUSTNESS EVALUATION

In Stage B, we have significantly reduced the loss of encoding messages. However, there may still exist few error modules in

²The experimental results are detailed in Section VII-B.

TABLE II
THE REFINEMENT FOR FEATURES RECONSTRUCTION LAYERS

Layers of Style Feature Reconstruction Loss	
[16]	relu1_2 , relu2_2 , relu3_3 , relu4_3
Ours	relu1_2 , relu2_1 , relu3_1 , relu4_3
Layers of Content Feature Reconstruction Loss	
[16]	relu3_3
Ours	relu1_2 , relu2_1 , relu3_1 , relu4_3

Q_b . Thus, we present a module based robustness-optimization mechanism in this stage to independently detect and correct each error module by balancing the robustness and visual quality, which leads to a robust art style result Q_c .

A. Basic of Reading QR Code

QR code is based on the rules of RS code, which cannot be decoded once sampled errors data exceed the error-correction capability. To address this issue, we divide the translating process of QR code messages into two steps: *sampling* and *thresholding*. Note that a valid decoding of QR codes requires these two steps both correct.

For *sampling*, we follow the rules in ZXing [24] that is the most widely used library for QR code codec. ZXing rules that the sampled encoding message is only related to each module's center pixel. Following this rule, the sampled center pixels of all modules are further grayed and thresholded after the encoding area is determined by the finder/alignment patterns.

For *thresholding*, we define a thresholding function ψ to convert the grayscale sampled pixels Q_x^g into binary format Q_x^b .

$$Q_x^b = \psi(Q_x^g, Q_x^t) = \begin{cases} 1, & \text{if } Q_x^g \in [Q_x^t, 255] \\ 0, & \text{if } Q_x^g \in [0, Q_x^t] \end{cases}, \quad (8)$$

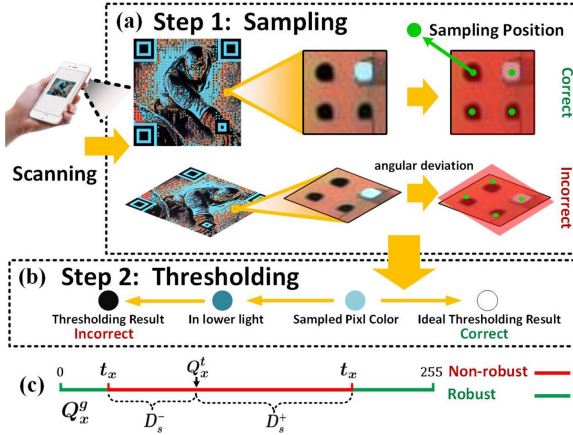


Fig. 10. (a) For sampling step, collected pixels may incorrect by external factors, e.g., scanning distance, angle tilt, poor camera resolution. (b) For thresholding step, sampled pixels may be thresholded incorrectly by external factors, e.g., brightness, light's color. (c) To evaluate the robustness of pixel x , we set a finite interval, called non-robust region, in both positive and negative directions of Q_x^t on the gray value axis.

where Q_x^g , Q_x^t , Q_x^b are gray value, threshold, and binary results of pixel x , respectively. According to ZXing, the threshold Q_x^t is not a constant and computed by a *mean block binarization method* proposed in [4], [23].

B. Robustness Evaluation of Encoding Modules

In this subsection, we introduce how to estimate modules' robustness in our module based robustness-optimization mechanism. Following the two steps aforementioned, we evaluate the system robustness on sampling and thresholding. In reality, the translated message may differ from the ideal, due to the external factors (for sampling, e.g., image zoom, angle tilt, poor camera resolution; for thresholding, e.g., brightness, light's color). We can reduce the detriments of these factors by adapting the controllable attributes of QR codes, i.e., the modules' sizes and the modules' colors for optimizing the sampling [cf. Fig. 10(a)] and thresholding [cf. Fig. 10(b)] steps respectively.

For the robustness of sampling, Chu *et al.* [7] proved that decoding a module of size $a \times a$ correctly requires an area at least $\frac{1}{3}a \times \frac{1}{3}a$ size in module's center contains the correct information. Intuitively, for the k -th module M_k of the target QR code, in our setting, we employ a circular spot $S_{(k, \frac{1}{4}a)}$ of radius $\frac{1}{4}a$ pixels concentric with M_k as a unit carrying the encoding messages. Our motivation to employ the encoding unit $S_{(k, \frac{1}{4}a)}$ is that the circular spot ensures the sampled pixels are the same in various scanning angles. Meanwhile, the size of $S_{(k, \frac{1}{4}a)}$ is larger than that of the theoretical valid size of module aforementioned in [7]. In addition, considering the dynamic requirements of aesthetic quality and robustness, we offer a configurable radius of the spot for users (cf. Fig. 16).

For the robustness of thresholding, given a QR code Q , the sampled threshold is distributed around the optimal threshold Q_x^t due to the extraneous factors such as brightness and light color. In fact, the closer Q_x^g to the ideal boundary (0 or 255), the higher probability of Q_x^g thresholding correctly (cf. Fig. 10(c)).

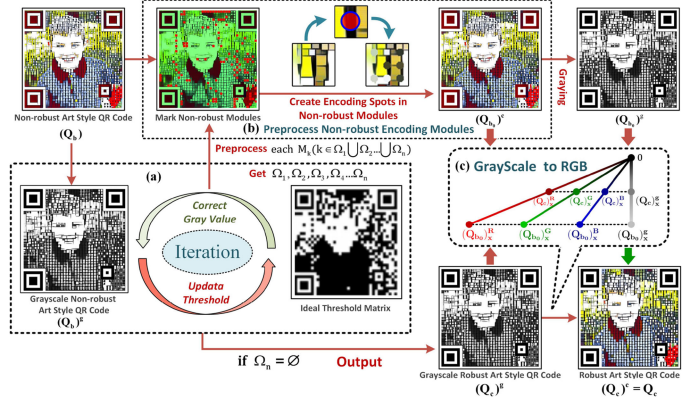


Fig. 11. Flowchart of Stage C. (a) Correcting non-robust modules, and updating thresholds, iteratively, until each module is robust. (b) Preprocessing non-robust modules by creating encoding spots. (c) Transforming grayscale robust art style QR code to RGB color and produce Q_c finally.

Accordingly, we next describe how to evaluate the robustness of module M_k in Q . ZXing shows only the central pixels of modules influence the sampling results, which indicates the pixels closer to the center are more important. Hence, we define function R_{M_k} by *Gauss weight function* $G_{M_k}(x)$ to compute the robustness of M_k ,

$$R_{M_k} = \sum_{x \in M_k} \xi(Q, x) \cdot G_{M_k}(x), \quad (9)$$

where $G_{M_k}(x)$ is same as Eq.(3). $\xi(Q, x)$ is used to evaluate whether the pixel x satisfies the robustness requirement under the constraint parameter δ ,

$$\xi(Q, x) = 1 - [Q_x^i \oplus \psi(Q_x^g, t_x)], \quad (10)$$

and t_x is calculated by

$$t_x = \begin{cases} Q_x^t + D_s^+, & \text{if } Q_x^i = 1 \\ Q_x^t - D_s^-, & \text{if } Q_x^i = 0 \end{cases}, \quad (11)$$

where Q_x^i is the ideal thresholding result of Q_x^g , $D_s^- = \delta |Q_x^t|$ and $D_s^+ = \delta |255 - Q_x^t|$ represent non-robust region in the positive/negative direction respectively (cf. Fig. 10(c)). Q_x^i is obtained by

$$Q_x^i = \begin{cases} (Q_s)_x^b, & \text{if } x \in \{S_{(1,r)}, S_{(2,r)} \dots S_{(\infty,r)}\} \\ Q_x^b, & \text{otherwise} \end{cases}, \quad (12)$$

where $(Q_s)_x^b$ and Q_x^b are the thresholding results of pixel x in standard QR Code Q_s and Q respectively. Finally, $R_{M_k} \geq \eta$ or $R_{M_k} < \eta$ means M_k is classified as a robust or non-robust module. The value of η is set to 0.8 empirically.

C. Module Based Robustness Optimization

As illustrated in Fig. 11, our module based robustness-optimization mechanism contains three main components: i) preprocessing non-robust modules in Q_b ; ii) iterative-update based error correction; iii) transforming grayscale to RGB color.

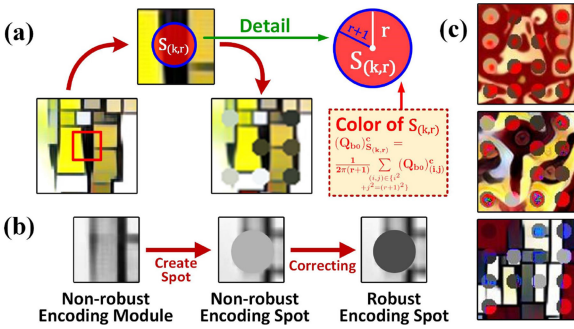


Fig. 12. (a) Specific steps of preprocessing non-robust modules in Q_b , where the color of $S_{(k,r)}$ is computed by Eq. (13). (b) Specific steps that correcting a grayscale non-robust encoding module. (c) The output Q_c without processing by (a), i.e., the corrected spots have serious visual-unpleasant artifacts.

1) *Preprocessing Non-Robust Modules in Q_b* : A serious issue is that the corrected encoding spots in Q_c may incur visual-unpleasant artifacts during the process of correcting Q_b [cf. Fig. 12(c)]. Aiming at solving this problem, we preprocess Q_b to obtain Q_{b0} via constructing spot in each non-robust module of Q_b [cf. Figs. 11(b) and 12(a)]. The color of each encoding spot $S_{(k,r)}$ in non-robust module M_k is computed by

$$(Q_{b0})_{S_{(k,r)}}^c = \frac{1}{2\pi(r+1)} \sum_{\substack{(i,j) \in \{i\}^2 \\ + j^2 = (r+1)^2}} (Q_{b0})_{(i,j)}^c, \quad (13)$$

where i, j are defined by Eq. (3), Q_{b0} is utilized as the reference image that assists in transforming the grayscale $(Q_c)^g$ to colored $(Q_c)^c$.

2) *Transforming Grayscale to RGB Color*: After we correct all error modules by an *iterative update based robustness optimization algorithm*³ to obtain the robust grayscale art style QR code $(Q_c)^g$, our task is to convert the grayscale $(Q_c)^g$ into the colored $(Q_c)^c$ [cf. Fig. 12(c)]. Let $\zeta_{Q_x^c} = [Q_x^R, Q_x^G, Q_x^B]^T$ denote the color in RGB space of Q_x^c , where Q_x^R, Q_x^G, Q_x^B represent the color values of pixel x in R, G, B channels respectively. Here, we adopt a widely used formula

$$Q_x^g = \alpha Q_x^R + \beta Q_x^G + \gamma Q_x^B, \quad (14)$$

to calculate the grayscale value, where $\alpha = 0.299$, $\beta = 0.587$, $\gamma = 0.114$, and Q_x^g is the gray value of a pixel x in grayscale QR code Q^g . We also construct a vector $\kappa = (\alpha, \beta, \gamma)$ to deform Eq. (14) into:

$$Q_x^g = \kappa \zeta_{Q_x^c}. \quad (15)$$

Afterwards, let θ to denote the ratio of robust grayscale QR code $(Q_c)^g$ to the non-robust one $(Q_{b0})^g$, in pixel x , as

$$\theta = \frac{(Q_c)_x^g}{(Q_{b0})_x^g} = \frac{\kappa \zeta_{(Q_c)_x^c}}{\kappa \zeta_{(Q_{b0})_x^c}}. \quad (16)$$

Combining Eq. (15) and Eq. (16), we obtain

$$\zeta_{(Q_c)_x^c} = \theta \zeta_{(Q_{b0})_x^c}. \quad (17)$$

³The algorithm can be found in Appendix B.

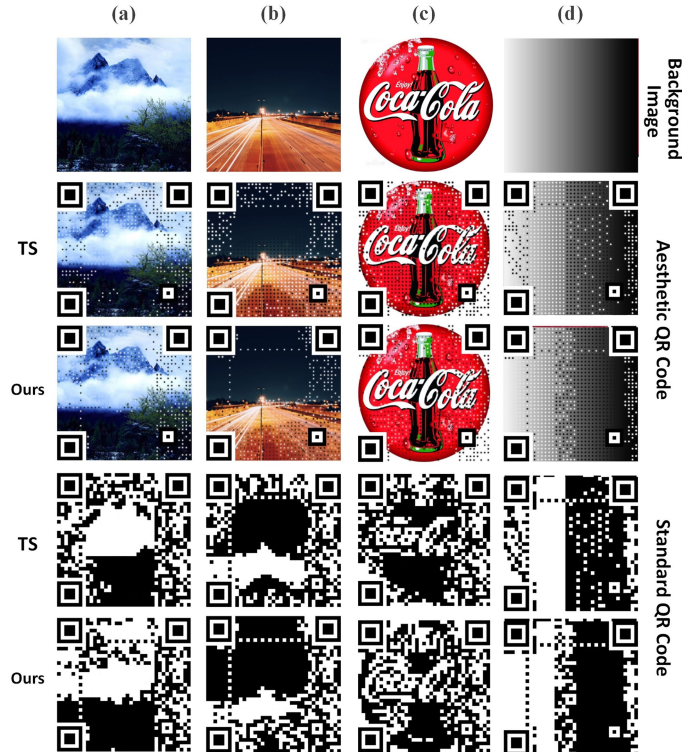


Fig. 13. Comparison of experimental results between our Q_a and TS (TS is the results of Two-Stage based method in [10]). Our results focus on the global feature of the blended image I , and the black/white encoding modules preferentially assigned to the darker/lighter color in I , which minimizes the visual contrast between noise-like modules and I .

Therefore, we can get RGB color of each pixel in Q_c , meanwhile, $(Q_c)^c$ and $(Q_c)^g$ satisfy the conversion relation in Eq. (14), that is, $(Q_c)^c$ is as robust as $(Q_c)^g$.

VII. EXPERIMENT

We conduct experiments on Q_a , Q_b , and Q_c respectively. The experimental processes and results are described as follows three subsections.

A. Experiments on Q_a

1) *Experimental Configuration of Q_a* : To evaluate the performance of TS [10] and our method, we prepare a dataset D which contains 300 images of 512×512 pixels with various contents (e.g., landscapes, cartoons, animals, characters, and trademarks). All images in D are indexed from 1 to 300 and used as blended images for generating baseline aesthetic QR codes Q_a .

2) *Comparison of Structure Similarity*: We adopt a *Structural SIMilarity (SSIM)* index proposed in [25] to measure the similarity between two images. Let $SSIM(M)$ denote the *SSIM* index between the produced QR code and the corresponding blended image by M (M denotes TS or our method). Here, $SSIM(M)$ ranges from -1 to 1 , $SSIM(M) = 1$ means the aesthetic QR code is the same as the blended image. As shown in Fig. 13, in our results, the black/white modules are preferentially assigned to the locations with darkest/lightest color of

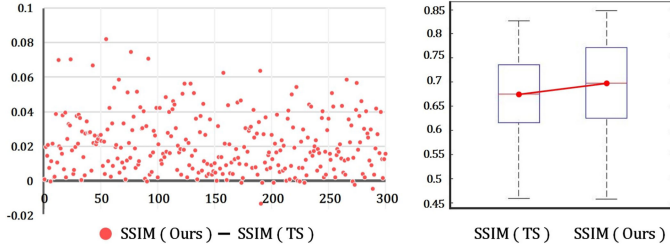


Fig. 14. We experiment on indexed 1 to 300 blended images in dataset D, and produce baseline aesthetic QR codes by method TS [10] and ours respectively. Left: The scatter-plot shows the resultant values of $SSIM(Ours)$ subtracts $SSIM(TS)$. Right: The box-plot shows the results of $SSIM(Ours)$ and $SSIM(TS)$. The experimental results illustrate that our method outperforms TS in the visual effect.

the blended images, which effectively reduces the visual noise. Fig. 14 shows that the results of $SSIM(Ours)$ subtracts $SSIM(TS)$ are positive in 96.3% cases, which means our method outperforms TS in the visual effect.

B. Experiments on Q_b

1) *Experimental Configuration of Q_b :* We train the adapted style transfer network and the original one [17] on MS-COCO dataset [26]. Employing each of the two networks, we generate 300 Q_b via combining 10 style target images⁴ and the 300 content target images Q_a (output from the *Experiment on Q_a*) respectively.

2) *Comparisons of Visual Quality and Robustness:* The visual comparison between the results generated by the original style transfer system [17] and our refined one respectively, as shown in Fig. 3 of the Appendix. It can be found the baseline system used in [17] excessively focuses on the high-level features, which is easily affected by the dense encoding modules and result in serious messy color blocks in outputs when Q_a is as the content target. These messy color blocks significantly affect the visual quality and weaken the robustness of Q_b .

Aiming at evaluating the improvement on robustness, we calculate the average number of error modules in two situations: i) For 10 kinds of styles, each of them combines with 300 content target images respectively (evaluating the universal validity of each style); ii) For 300 content target images, each of them combines with 10 kinds of styles respectively (evaluating the universal validity of each content target). The experimental results as shown in Fig. 15, the average error-modules number of our results are approximate 60% of the baseline system in both two situations.

To sum up, we make the style transformation system suitable for beautifying the baseline aesthetic QR code, which significantly improves the visual quality and robustness of Q_b .

C. Experiments on Q_c

We evaluate the robustness and visual quality of Q_c in following experiments.

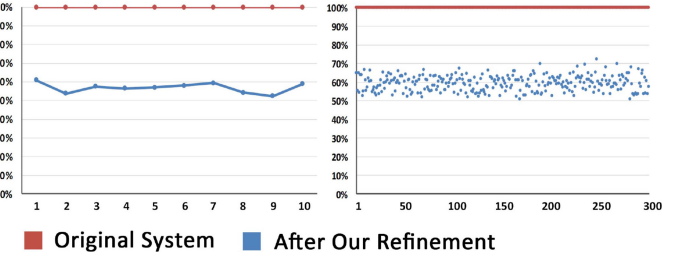


Fig. 15. **Left:** The 100% Stacked Line Chart displays the average numbers of error-modules in results, which produced by 10 styles (indexed from 1 to 10), and each of them combine with 300 content target images respectively (indicating the universal validity of each style). **Right:** The 100% Stacked Scatter Chart, displays the average numbers of error-modules in results, which produced by 300 content target images (indexed from 1 to 300), and each of them combine with 10 styles respectively (indicating the universal validity of each content target). Experimental results show that the error-modules number in our result are approximate 60% of original system in both two situations, which means our refinement works well in robustness enhancing.

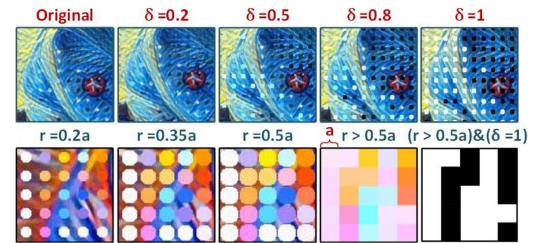


Fig. 16. The appearance changes of Q_c with different δ and r . δ and r control modules' colors and sizes respectively. A larger δ or r makes Q_c more robust, and a smaller δ or r makes Q_c more similar to Q_b that has higher visual quality.

1) *Influence of δ and Radius r :* As mentioned in subsection B of Section VI, varying parameters δ and r is important for users to balance the performance of visual quality and robustness. As shown in the results (cf. Fig. 16), a larger δ or r incurs more noise-like encoding spots in Q_c , which reduces the visual quality yet enhances the robustness.

2) *Visual Quality Evaluation:* We conduct a user survey to evaluate the subjective visual quality. Preparing for the experiment, we randomly select 6 images from D as the blended images to generate 6 group of QR codes. Each group includes 8 images: 4 SEE QR codes in different styles generated by us and 4 aesthetic QR codes of others (e.g., Visualead QR code (VS) [6], Halftone QR code (HF) [7], Efficient QR code (EF) [8], and Two-Stages QR Code (TS) [10]). The produced QR codes corresponding to each method can be found in Fig. 4 of Appendix C, each image is of size 512×512 pixels and the version number of the QR code is 5.

We invited 40 volunteers (25 males and 15 females) irrelevant to this work to conduct two user studies: 1) scoring each group on a level of 1 to 5 (cf. Table III); 2) voting on that they prefer generating QR code in “fixed styles” or “diverse styles”. The result of user studies as shown in Fig. 17, we can find that the visual quality of our SEE QR Code has reached the state-of-the-art level. Besides, our work does better in personalized and diversity, which caters to almost all users’ wishes and outperforms other state-of-the-art works.

⁴The style target images can be found in Fig. 2 of Appendix C.

TABLE III
THE MEANING OF EACH GRADE

Grade	Indicate
5	very satisfied
4	satisfied
3	common
2	dissatisfied
1	very dissatisfied

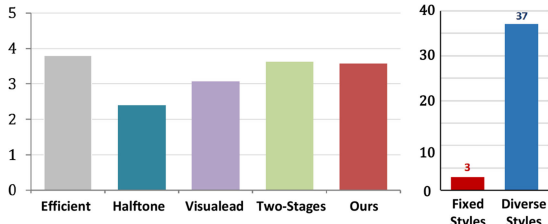


Fig. 17. **Left:** the result of the subjective test on attractiveness, which illustrates our SEE QR code reaches the state-of-the-art level in visual quality (we use the average score of 4 different styles as our final score). **Right:** voting results of people desire to produce QR codes in fixed styles or diverse styles. 92.5% of participants want to have more style choices of QR codes, and our method effectively satisfies this demand and outperforms other state-of-the-art works.

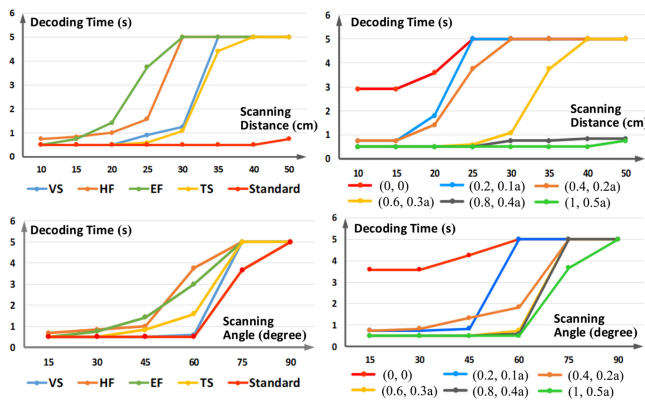


Fig. 18. Comparison experiments on different scanning distances and angles. **Top left and bottom left:** Results of existing works. **Top right and bottom right:** Our results under different (δ, r) setting. For existing works, the modifications of modules' sizes and colors make their codes have much poorer robustness than standard QR codes, yet, our work can effectively control robustness by different setting, and when $\delta = 1, r = 0.5a$, our codes achieve the best robustness that equal to standard QR codes.

3) *Robustness Evaluation:* First, we conduct a comparison experiment to estimate the robustness in different scanning distances and angles. In the experiment, we show a $5\text{cm} \times 5\text{cm}$ QR code on the screen, someone uses a mobile device to scan this code in varying distances and angles. The decoding time is defined as the time that QR code reader returns a correct data, and each decoding time is divided into the nearest one in $\{0.5\text{s}, 1\text{s}, 1.5\text{s}, \dots, 3\text{s}\}$, and we record the time exceeded 3 seconds as 5 seconds which means unreadable. For each work, we calculated the average of 6 examples' scan times as the final results. As shown in Fig. 18, compared with the standard QR Codes, existing works' results have poorer robustness, yet, our robust optimization mechanism can effectively control robustness by

TABLE IV
DECODING RATES ON DIFFERENT MOBILE DEVICES

Mobile Phone	App	Success Rate/Different Sizes		
		$(3\text{cm})^2$	$(5\text{cm})^2$	$(7\text{cm})^2$
Iphone 6s	Wechat	100%	100%	100%
	Neo Reader	100%	100%	100%
	Alipay	100%	100%	100%
	QR Code Reader	100%	100%	100%
Huawei Honor 7	Wechat	100%	100%	100%
	Neo Reader	100%	100%	100%
	Alipay	100%	100%	100%
	QR Code Reader	100%	100%	100%
Samsung Note 8	Wechat	100%	100%	100%
	Neo Reader	98%	100%	100%
	Alipay	100%	100%	100%
	QR Code Reader	100%	100%	100%
Xiaomi Note 3	Wechat	100%	100%	100%
	Neo Reader	96%	100%	100%
	Alipay	100%	100%	100%
	QR Code Reader	100%	100%	100%

different setting, and when $\delta = 1, r = 0.5a$, our codes achieve the best robustness that almost equal to the standard QR codes. It should be noted that some cases are readable when $\delta = 0, r = 0$ because of our tailored style transfer network can remain many modules' readability.

Second, we design an experiment to evaluate the robustness of Q_c in different mobile devices and QR code readers. We examine the robustness on 4 group of our SEE QR code which used in the experiment of *visual quality evaluation*. Meanwhile, considering the influence of image size on decoding performance, we scan each example with size $3\text{cm} \times 3\text{cm}$, $5\text{cm} \times 5\text{cm}$, and $7\text{cm} \times 7\text{cm}$, in the distance of 20cm, respectively, by different mobile phones and QR decoders. The successful decoding rate is calculated via $\frac{\text{Successful decoding times}}{\text{Scanning times}} \times 100\%$ in 50 scanning times.

As shown in Table IV, the successful decoding rates are always greater than 96%, which means our SEE QR code is robust enough for daily applications. In addition, users can also enhance the resultant robustness by increasing δ or r with sacrificing little visual quality.

VIII. CONCLUSION

In this paper, we propose a novel automatic approach equipping with a module based robustness-optimization mechanism to generate beautiful art style QR code called *SEE QR code*. Compared with the state-of-the-art, our SEE QR code achieves better performance in the perspectives of personalization, artistry, and robustness, which can efficiently support the real-life application and business promotion.

REFERENCES

- [1] T. Wakahara and N. Yamamoto, "Image processing of 2-dimensional barcode," in *Proc. Int. Conf. Netw.-Based Inf. Syst.*, Sep. 2011, pp. 484–490.
- [2] D. Samretwit and T. Wakahara, "Measurement of reading characteristics of multiplexed image in QR code," in *Proc. 3rd Int. Conf. Intell. Netw. Collaborative Syst.*, 2011, pp. 552–557.

- [3] Y.-S. Lin, S.-J. Luo, and B.-Y. Chen, "Artistic QR code embellishment," *Comput. Graph. Forum*, vol. 32, no. 7, pp. 137–146, 2013.
- [4] G. J. Garateguy, G. R. Arce, D. L. Lau, and O. P. Villarreal, "QR images: Optimized image embedding in QR codes," *IEEE Trans. Image Process.*, vol. 23, no. 7, pp. 2842–2853, Jul. 2014.
- [5] A. Falcon, 40 gorgeous QR code artworks that rock, 2013. [Online]. Available: <http://www.hongkiat.com/blog/qr-code-artworks>
- [6] N. Aliva, U. Peled, and F. Itamar, "Visualead," 2012. [Online]. Available: <http://www.visualead.com>
- [7] H. K. Chu, C. S. Chang, R. R. Lee, and N. J. Mitra, "Halftone QR codes," *ACM Trans. Graph.*, vol. 32, no. 6, 2013, Art. no. 217.
- [8] S.-S. Lin, M.-C. Hu, C.-H. Lee, and T.-Y. Lee, "Efficient QR code beautification with high quality visual content," *IEEE Trans. Multimedia*, vol. 17, no. 9, pp. 1515–1524, Sep. 2015.
- [9] Y.-H. Lin, Y.-P. Chang, and J.-L. Wu, "Appearance-based QR code beautifier," *IEEE Trans. Multimedia*, vol. 15, no. 8, pp. 2198–2207, Dec. 2013.
- [10] Y. Zhang, S. Deng, Z. Liu, and Y. Wang, "Aesthetic QR codes based on two-stage image blending," in *Proc. Int. Conf. Multimedia Model.*, 2015, pp. 183–194.
- [11] M. Xu *et al.*, "Art-up: A novel method for generating scanning-robust aesthetic qr codes," 2018, arXiv:1803.02280.
- [12] M. Kuribayashi and M. Morii, "Aesthetic QR code based on modified systematic encoding function," *IEICE Trans. Inf. Syst.*, vol. E100.D, no. 1, pp. 42–51, 2017.
- [13] C. Fang, C. Zhang, and E.-C. Chang, "An optimization model for aesthetic two-dimensional barcodes," in *Proc. Int. Conf. Multimedia Model.*, 2014, pp. 278–290.
- [14] R. Cox, "Qartcodes," 2012. [Online]. Available: <http://research.swtch.com/qart>
- [15] L. A. Gatys, A. S. Ecker, and M. Bethge, "Image style transfer using convolutional neural networks," in *Proc. IEEE Conf. Comput. Vis. Pattern Recognit.*, 2016, pp. 2414–2423.
- [16] C. Li and M. Wand, "Combining Markov random fields and convolutional neural networks for image synthesis," in *Proc. IEEE Conf. Comput. Vis. Pattern Recognit.*, 2016, pp. 2479–2486.
- [17] J. Johnson, A. Alahi, and F.-F. Li, "Perceptual losses for real-time style transfer and super-resolution," in *Proc. Eur. Conf. Comput. Vis.*, 2016, pp. 694–711.
- [18] D. Ulyanov, V. Lebedev, A. Vedaldi, and V. Lempitsky, "Texture networks: Feed-forward synthesis of textures and stylized images," in *Proc. Int. Conf. Machine Learning.*, 2016, pp. 1349–1357.
- [19] D. Chen, L. Yuan, J. Liao, N. Yu, and G. Hua, "StyleBank: An explicit representation for neural image style transfer," in *Proc. IEEE Conf. Comput. Vis. Pattern Recognit.*, 2017, pp. 2770–2779.
- [20] J. Liao, Y. Yao, L. Yuan, G. Hua, and S. B. Kang, "Visual attribute transfer through deep image analogy," *ACM Trans. Graph.*, vol. 36, no. 4, 2017, Art. no. 120.
- [21] Information Technology Automatic Identification and Data Capture Techniques Code Symbology QR Code, ISO/IEC 18004:2000.
- [22] K. Simonyan and A. Zisserman, "Very deep convolutional networks for large-scale image recognition," 2014, arXiv:1409.1556.
- [23] O. Russakovsky *et al.*, "Imagenet large scale visual recognition challenge," *Int. J. Comput. Vis.*, vol. 115, no. 3, pp. 211–252, 2015.
- [24] ZXing, 2013. [Online]. Available: <https://github.com/zxing/zxing>
- [25] Z. Wang, A. C. Bovik, H. R. Sheikh, and E. P. Simoncelli, "Image quality assessment: From error visibility to structural similarity," *IEEE Trans. Image Process.*, vol. 13, no. 4, pp. 600–612, Apr. 2004.
- [26] T. Y. Lin *et al.*, "Microsoft COCO: Common objects in context," in *Proc. Eur. Conf. Comput. Vis.*, 2014, vol. 8693, pp. 740–755.

Authors' photographs and biographies not available at the time of publication.